Biometals
https://doi.org/10.1007/s10534-020-00260-2

Metabolomics analysis of the effects of quercetin on renal toxicity induced by cadmium exposure in rats

Tong Guan · Youwei Xin · Kai Zheng · Ruijuan Wang · Xia Zhang · Siqi Jia · Siqi Li · Can Cao · Xiujuan Zhao

Received: 7 July 2020 / Accepted: 1 October 2020

Abstract This study aims to explore the protective effects of quercetin against cadmium-induced nephrotoxicity utilizing metabolomics methods. Male Sprague–Dawley rats were randomly assigned to six groups: control, different dosages of quercetin (10 and 50 mg/kg·bw, respectively), CdCl2 (4.89 mg/kg·bw) and different dosages quercetin plus CdCl2 groups. After 12 weeks, the kidneys were collected for metabolomics analysis and histopathology examination. In total, 11 metabolites were confirmed, the intensities of which significantly changed (up-regulated or down-regulated) compared with the control group ($p < 0.00067$). These metabolites include xanthosine, uric acid (UA), guanidinosuccinic acid (GSA), hypoxanthine (Hyp), 12-hydroxyeicosatetraenoic acid (tetranor 12-HETE), taurocholic acid (TCA), hydroxyphenylacetylglycine (HPAG), deoxyinosine (DI), ATP, formiminoglutamic acid (FIGLU) and arachidonic acid (AA). When high-dose quercetin and cadmium were given to rats concurrently, the intensities of above metabolites significantly restored ($p < 0.0033$ or $p < 0.00067$). The results showed quercetin attenuated Cd-induced nephrotoxicity by regulating the metabolism of lipids, amino acids, and purine, inhibiting oxidative stress, and protecting kidney functions.

Keywords Cadmium · Quercetin · Metabolomics · UPLC-MS · Nephrotoxicity

Introduction

Cadmium (Cd) is a toxic heavy metal pollutant generally distributed in the environment, mainly existed in air, mining, smelting, electroplating, phosphate fertilizer and sludge (Tian et al. 2020; Turner 2019). Due to numerous industrial and human activities, environmental pollution is inevitable. For the non-occupational population, cadmium exposure is primarily through food, water, air, and dust (Bartholomew et al. 2020; Lamtai et al. 2020). In addition, smoking is another important way for the general population to contact cadmium. Cadmium, with an exceptionally long biological half-life of 10 to 30 years, is the most easily accumulated toxic substance in the body (Järup and Akesson 2009). Long-

Electronic supplementary material The online version of this article (https://doi.org/10.1007/s10534-020-00260-2) contains supplementary material, which is available to authorized users.

T. Guan · Y. Xin · K. Zheng · R. Wang · X. Zhang · S. Jia · S. Li · C. Cao (✉) · X. Zhao (✉)
Department of Nutrition and Food Hygiene, Public Health College, Harbin Medical University, 194 Xuefu Road, Harbin 150081, Heilongjiang, China
e-mail: 103037287@qq.com

X. Zhao
e-mail: xiujuan_zhao@sina.com

Published online: 08 October 2020

term intake can cause different degrees of damages to the body.

Studies have found that Cd exposure had many impacts on metabolism, such as mitochondrial energy metabolism, amino acid metabolism, phospholipid metabolism, purine metabolism, intestinal flora metabolism, bile acid metabolism, tricarboxylic-acid cycle, etc. (Chen et al. 2018; Hu et al. 2018). And Cd exposure can also lead to lung, kidney, pancreatic and prostate cancers (Djordjevic et al. 2019). The International Agency for Research on Cancer (IARC) has classified cadmium as the first class of carcinogens. It is widely reported in populations and diverse experimental models that the kidney is a key target of chronic Cd exposure. Numerous studies have demonstrated that the pathological biochemical mechanism of renal damage caused by cadmium is carried out mainly through the induction of oxidative stress (Sun et al. 2019). Cadmium indirectly produces reactive oxygen species (ROS) after entering human cells, alters renal endogenous antioxidant status, and causes peroxidative damage to biofilm lipids and DNA, eventually leads to apoptosis, has a certain damage to the kidney (Ghosh and Indra 2018; Joardar et al. 2019). Therefore, reducing the harm of cadmium to human body especially the target organ kidney should be paid more and more attention.

Quercetin (QE) is a typical flavonoid, ubiquitously found in onions, peppers, blueberries, apples, cherries and other fruits and vegetables (Mao et al. 2018). It has various kinds of physiological activities, such as antioxidation, anti-inflammation, immune regulation and so on (Ou et al. 2020; Roy et al. 2018). Many studies have found quercetin can regulate the intestinal microflora and various metabolic pathways, including tricarboxylic-acid cycle and energy metabolism, bile acid, amino acid and nucleic acid metabolism (Zhang et al. 2018). In recent years, the protective effects of quercetin on toxicity induced by exogenous harmful substances have attracted increased attention (Pingili et al. 2020). Studies have demonstrated that quercetin can prevent oxidative damage induced by cadmium through scavenging oxygen free radicals, reducing the lipid peroxidation, improving intracellular antioxidant status and inhibiting apoptosis (Mao et al. 2018; Pingili et al. 2020). However, most of these studies focused only on the level of tissues or organs, few have been reported to study the protective effects from the metabolic level of the organism.

Metabolomics is defined as "quantitative measurement of dynamic multiparameter metabolic responses of the life system to pathophysiological stimuli or genetic modifications" (Xu et al. 2019b). Metabolomics is usually performed on biological samples (such as serum, urine, stool, tissues, etc.), and can provide a comprehensive view of the whole system biology. As an emerging analytical tool, metabolomics has been widely used in food safety assessment, drug development, disease diagnosis, environmental contamination evaluation and other fields in recent years (García-Sevillano et al. 2015; Griffin 2020; Su et al. 2019).

In a previous work, we have reported the effects of quercetin on cadmium-induced toxicity in rat urine by metabolomics methods, and the results showed that quercetin had a partial protective effect on cadmium-induced nephrotoxicity (Liu et al. 2019). However, the protective mechanism of quercetin remains unclear. Therefore, this study used metabolomics techniques to analyze rat kidneys, and comprehensively explained the protective mechanism of quercetin against Cd in combination with previous urine results.

Materials and methods

Chemicals and reagents

Cadmium chloride (99.99% purity) and quercetin (98% purity) were purchased from Sigma-Aldrich (Germany). High-performance liquid chromatography (HPLC) grade methanol and acetonitrile were obtained from Dikma Science and Technology, Co. Ltd. (Ontario, Canada). And HPLC grade formic acid was purchased from Beijing Reagent Company (Beijing, China). Leucine enkephalin was supplied by Sigma-Aldrich (St. Louis, MO, USA). Assay kits for creatinine (CRE), blood urea nitrogen (BUN), and uric acid (UA) were obtained from Wako Pure Chemical Industries Ltd. (Nagoya, Japan). The ELISA Kits for phospholipase A2 (PLA2) were purchased from Jiangsu Jingmei Biological Technology Co. Ltd (Jiangsu, China) and glutathione peroxidase (GPx) kits were purchased from Nanjing Jiancheng Bioengineering Institute (Nanjing, China). Carboxymethylated cellulose (CMC) and other chemicals used were of HPLC grade or reagent grade. Water was prepared using a Milli-Q water purification system (Millipore, Billerica, MA, USA).

Animals and experimental design

Sixty SPF-grade male Sprague–Dawley rats (weighing 180 ± 20 g) were procured from Vital Laboratory Animal Technology Co. Ltd (Beijing, China). The rats were fed adaptively for a week before be used. The rats were housed singly in cages with free access to American Institute of Nutrition (AIN)-93M rodent diets and distilled water in a temperature-controlled facility (equivalent temperature 22 ± 2 °C, relative humidity 50–60%, natural 12-h/12-h light/dark cycle). The whole animal experiment process conformed to the guide for the care and use of laboratory animals of Harbin Medical University (Heilongjiang, China), and had been approved by the medical ethics committee of Harbin Medical University.

After an initial habituation period of 7 days, 60 rats were randomly allocated to six groups of 10 rats in each: control group (C), low-dose quercetin treatment group (Q1), high-dose quercetin treatment group (Q2), cadmium treatment group (D), Cd plus low-dose quercetin treatment group (DQ1) and Cd plus high-dose quercetin treatment group (DQ2). The dose of cadmium (4.89 mg/kg·bw) was determined from previous studies, indicating obvious toxic effects in rats (Liu et al. 2019). Cadmium chloride was dissolved in distilled water and given to rats in groups D, DQ1 and DQ2 through daily drinking, whereas rats in groups C, Q1 and Q2 were simply given distilled water in the same way. The low-dose quercetin treatment group (10 mg/kg bw/day) and the high-dose quercetin treatment group (50 mg/kg·bw/day) were determined respectively based on the minimum intake (5.96 mg/day) and the maximum intake (29.4 mg/day) of quercetin in the population (Zhang et al. 2010). Quercetin was dissolved in 0.5% CMC and given to rats in groups Q1, Q2, DQ1 and DQ2 by oral gavage once per day, while rats in C and D groups were treated with intragastric injection of 0.5% CMC. Body weight was weighed weekly and water consumption of each rat was recorded daily during the experimental period of 12 weeks. Throughout the whole experiment, no significant differences were observed in water consumption among all groups at each time point ($p > 0.05$) (Liu et al. 2019).

Sample collection and preparation

Rat serum collection and preparation

After the experiment completed, rats were anesthetized with intraperitoneal (i. p.) injection of 10% chloral hydrate (3 ml/kg·bw). Blood samples were collected from the abdominal artery using coagulation-promoting tubes and then centrifuged at 3000 rpm for 15 min at 4 °C. The supernatants (serum) were used for metabolomics analysis (Jia et al. 2020) using UPLC-MS, and biochemical indicators (CRE, BUN, and UA) detection using Hitachi 7100 automated biochemical analyzer (Hitachi Co. Japan).

Rat kidney collection and preparation

After the rats were sacrificed, the kidneys were dissected out, weighed, and washed using 0.9% NaCl. One kidney of each rat was placed in 10% formalin for subsequent histopathology analyses. The rest of the kidney tissues were wrapped in tin-foil, immediately snap-frozen in liquid nitrogen and stored at − 80 °C for metabolomics analysis and subsequent associated enzyme activities (PLA2, GPx) and cadmium content detection.

Before analysis, 0.1 g kidney tissues were weighed and then homogenized using a homogenizer containing chloroform (600 μL), methanol (600 μL), distilled water (400 μL). After homogenization, the samples were vortexed and placed on ice for 10 min, followed by centrifugation at 12,000 rpm at 4 °C for 10 min (Allegra^{TM} 64 R, Beckman, USA). Then the supernatants were collected, dried in a vacuum concentrator (CHRIST RCV2-25 CDplus) for 4 h. Before injection, the samples were re-dissolved with 280 μL distilled water and 120 μL acetonitrile (distilled water/acetonitrile = 7/3, V/V), and centrifuged again at 12,000 rpm for 10 min at 4 °C. The supernatants were collected for metabolomics analysis. Meanwhile, the stability and repeatability of the system were monitored using quality control (QC) sample. The QC sample was prepared by pooling equal aliquots (10 μL) from the 60 renal samples to contain a mean concentration of all analyzed metabolites, and every ten kidney samples injections were successively followed by one QC samples.

Measurement of Cd concentration in kidney

The concentration of Cd in kidneys was examined using atomic absorption spectrometer (AAS, Thermo Fisher Scientific; ICE 3500). 0.5 g samples were weighed and digested in conical flasks with 10 ml mixed acid ($HNO_3/HClO_4$ = 4/1, V/V) for 12 h. Subsequently, the samples were placed in a digestion furnace (KXL-1010) until the liquid turned colorless and transparent. After cooling, the liquids were transferred to colorimetric tubes and diluted to 10 ml with deionized water. Finally, the digestion solution was analyzed by AAS with a wavelength of 228.8 nm.

Determination of GPx and PLA2 activities in kidney

0.1 g kidney sample was homogenized with 900 μL 0.86% physiological saline, the homogenate was centrifuged at 3000 rpm for 10 min at 4 °C. The supernatant was collected to detect GPx activities according to the kit instructions.

0.1 g kidney sample was homogenized with 900 μL PBS, the homogenate was centrifuged at 3000 rpm for 20 min at 4 °C. The supernatant was collected to detect PLA2 activities according to the ELISA kit instructions.

Histopathological examinations

The kidney tissues were individually immersed in 10% formalin solution for at least 24 h. Dehydration was carried out according to standard procedures. Approximate 4 μm thick sections were prepared after embedded in paraffin wax. Standard light microscopy was performed after being stained with hematoxylin and eosin (HE).

Chromatography

Chromatographic separation was implemented on an HSS T3 column (100 mm × 2.1 mm, 1.8 μm i. d.; Waters Corporation., Milford, Massachusetts, USA) using a Waters' ACQUITY UPLC system (Waters Corp.). The temperatures of the autosampler and the column were set at 4 °C and 35 °C, separately. The UPLC mobile phases contained A (water with 0.1% formic acid) and B (acetonitrile). The gradient elution was 16 min at a flow rate of 0.45 mL/min. The protocols for the mobile phase gradient were applied as follows in the positive and negative ion modes: 0-2% B for 0–0.5 min; 2–5% B for 0.5–1 min; 5–12% B for 1–2 min; 12–20% B for 2–5 min; 20–32% B for 5–6.5 min; 32–45% B for 6.5–8.5 min; 45–65% B for 8.5–10 min; 65–98% B for 10–11 min; 98% B for 11–12 min; 98–30% B for 12–13 min; 30–2% B for 13–14 min; and 2% B for 14–16 min. A 2 μL aliquot of each sample solution was injected into the column.

Mass spectrometry

Mass spectrometry was carried out on a Xevo G2 Q-TOF mass spectrometer (Waters Corp, Milford, MA) equipped with electrospray ionization ion source in the positive (ESI^+) and negative (ESI^-) ion mode. The centroid data were obtained with the full scan mode from m/z 50–1000 for 0–16 min. The ESI source conditions were set as follows: desolvation gas (nitrogen, 900 L/h); cone gas (nitrogen, 50 L/h); desolvation temperature (450 °C); source block temperature (120 °C); capillary voltage (positive and negative ion modes were both 0.5 kV) and cone voltage (30 V). To ensure accuracy and reproducibility, a lock-mass of leucine enkephalin for positive ESI mode (m/z = 556.2771) and negative ESI mode (m/z = 554.2615) was used via a Lock Spray ^{TM} interface at a flow rate of 10 μL/min. The lock spray frequency was set at 10 s in the positive ion mode and 15 s in the negative ion mode.

Data processing and metabolite identification

The UPLC-MS data were analyzed using software Progenesis QI (version 2.1; Waters Corporation, Milford, MA). The metabolites were filtered according to one-way analysis of variance (ANOVA), p-value $<$ 0.05 and max fold change $\geq$ 2.

Then, a multivariate analysis of the data was carried out by using EZinfo statistical analysis software (version 2.0; Umetrics AB, Umeå, Sweden). Before multivariate statistical analysis, normalization and Pareto-scaling of the ion peaks were performed. To obtain a general overview of separation trends and verify the reproducibility and reliability of the method, unsupervised principal component analysis (PCA) was performed on all samples. The contribution of variables to each classification can be identified by corresponding loading plots. Then, supervised partial

least-squares discriminant analysis (PLS-DA) was used to further observe the discrimination between the groups and select potential metabolites. To avoid the over-fitting of supervised models, a cross-validation (seven folds) procedure and permutations test (200 iterations) were carried out using SIMCA-P software (version 12.0; Umetrics AB, Umea, Sweden). Parameters describing the variable importance in the projection (VIP) for each metabolite were calculated based on the PLS-DA model. VIP value reflects the contribution of every variable on the classification. Variables with VIP value > 1 have above-average influences on the classification of metabolites. Therefore, the metabolites with VIP value above 1.0 were selected for further study.

The selected metabolites were imported into Progenesis QI software again for metabolite identification. The Human Metabolome Database (HMDB) was used for the initial identification of metabolites, then multiple ambiguous identification for every compound was obtained. The confirmation of metabolites identified was based on the "Score", "Fragmentation score", and "Isotope similarity" given by Progenesis QI, and then the MS/MS fragmentation data from Progenesis QI software were further provided. The MS/MS spectra of metabolites were matched with the structure information from the Progenesis QI software. To reduce the false-positive identifications, structural confirmation was conducted by comparison with the standards (MS/MS spectrum). Open database sources, including the HMDB (https://www.hmdb.ca/), KEGG (https://www.kegg.com/), METLIN (https://metlin.scripps.edu) and MetaboAnalyst (https://www.metaboanalyst.ca/) were used to support the potential pathways of metabolites.

Statistical analysis

All statistical analyses were carried out using a computer software package (SPSS version 21.0; Beijing Stats Data Mining Co. Ltd, China). All results were expressed as mean $\pm$ standard deviations (SD). Differences between control and treatment groups were analyzed using ANOVA by post hoc LSD test when the data were normally distributed and the variance was homogenous. If not the non-parametric Kruskal–Wallis test was used. The statistical tests were considered to be significant at the $p < 0.05$ and highly significant at the $p < 0.01$ with 95% confidence interval. To determine the specificity and sensitivity of the metabolites to distinguish the treated groups from the control group, the area under the curve (AUC) value for receiver-operating characteristic (ROC) curve was calculated by using SPSS 21.0 software. Metabolites with AUC ≥ 0.9 had high accuracy and were selected as potential biomarkers (Xu et al. 2019a). To reduce the inflation of false positive rates due to multiple testing, Bonferroni correction ($p < 0.0033$ or $p < 0.00067$) was used to test for differences in the intensities of metabolites among six groups. A statistical correlation analysis was applied to normalize the intensities of metabolites found to be significantly different with Cd treatment to establish possible association between metabolites in the urine and kidneys. Pearson's correlation coefficients were computed between influential metabolite relative intensities derived from the urine and kidney metabolic profiles from the same rats with the same treatment (Feng et al. 2011).

Results

Impact of Cd or/and quercetin on biochemical parameters in serum

Serum CRE, UA and BUN are widely interpreted as indicators for assessing renal function in clinical practice today. At the end of the experiment, the biochemical parameters in serum were detected (Table 1). A significant ($p < 0.01$) increase in the level of UA, BUN and CRE in serum was observed in Cd-treated rats when compared with control group. Administration of high-dose quercetin along with Cd significantly ($p < 0.01$) restored the levels of UA, BUN and CRE when compared with Cd-alone-treated rats. There were significant differences in the above parameters between groups C and DQ2 ($p < 0.05$ or $p < 0.01$), while no significant differences among groups C, Q1 and Q2 or between groups D and DQ1 ($p > 0.05$).

Impact of Cd or/and quercetin on weights, Cd concentration and histological changes in kidney

After the 12 weeks of the experiment, the kidney of each rat was weighed, and the ratio of kidney weight to the corresponding total body weight (bw) (namely, the

Table 1 Biochemical parameters in serum

Groups	BUN (mmol/L)	UA (μmol/ L)	CRE (μmol/L)
C	6.63 ± 0.61	64.28 ± 3.00	35.36 ± 2.57
Q1	6.54 ± 0.75	63.57 ± 3.12	35.08 ± 1.79
Q2	6.55 ± 0.68	64.56 ± 3.68	35.13 ± 2.00
D	8.48 ± 0.59**	98.07 ± 3.73**	39.45 ± 2.21**
DQ1	8.34 ± 0.78**	96.58 ± 4.84**	39.34 ± 1.87**
DQ2	7.64 ± 0.55**##	81.81 ± 5.56**##	37.17 ± 1.17*##

Values expressed as mean ± SD (n = 10)

BUN blood urea nitrogen; *UA* uric acid; *CRE* creatinine; *C* control group; *Q1* low-dose quercetin-treated group; *Q2* high-dose quercetin-treated group; *D* Cd-treated group; *DQ1* low-dose quercetin plus Cd-treated group; *DQ2* high-dose quercetin plus Cd-treated group

*Significantly different from the control group at $p < 0.05$ (one-way ANOVA)

**Significantly different from the control group at $p < 0.01$ (one-way ANOVA)

#Significantly different from the Cd-treated group at $p < 0.05$ (one-way ANOVA)

##Significantly different from the Cd-treated group at $p < 0.01$ (one-way ANOVA)

kidney viscera coefficient) was calculated. As shown in Fig. S1, no significant difference was observed in the relative weights of the kidney between the groups ($p > 0.05$). Cadmium accumulation was measured in the kidneys according to the method of the National Food Safety Standard of the People's Republic of China (GB5009.15–2014). As shown in Fig. S2, the kidney Cd concentration in rats no exposed to Cd (groups C, Q1 and Q2) was under the limit of quantitative detection (0.003 mg/kg). Cd concentration of group D (235.74 ± 10.14 mg/kg tissue) significantly elevated compared with that of group C ($p < 0.01$), while the concentration of group DQ2 (140.06 ± 9.66 mg/kg tissue) significantly decreased compared with that of group D ($p < 0.01$). There was no significant difference in Cd concentration between group DQ1 (229.28 ± 14.24 mg/kg tissue) and D ($p > 0.05$). To determine renal toxicity, histopathologic analyses on the kidney were conducted. No significant histopathological changes were observed in the renal tissues of the control group and the different doses of quercetin treatment group (Fig. 1a–c, respectively). In group D and DQ1, there were pathological changes such as edema and vacuole degeneration of renal tubular epithelial cells, erythrocyte tubular type, nucleus swelling, mesangial cell and endothelial cell proliferation, interstitial inflammatory cell infiltration and so on (Fig. 1d–g, respectively). Histopathological changes in group DQ2 were relatively milder than those in groups D and DQ1, with only a small amount of swollen glomerulus existed (Fig. 1h).

Impact of Cd or/and quercetin on indicators related to metabolic pathways

The activities of PLA2 and GPx in the kidney are illustrated in Fig. 2. The activity of PLA2 significantly increased and GPx activity decreased in group D compared to those in group C ($p < 0.01$). After the administration of high-dose quercetin along with Cd, the activity of PLA2 significantly decreased and GPx activity significantly increased ($p < 0.01$), but there were still statistical differences from those in group C ($p < 0.01$).

Impact of Cd or/and quercetin on the changes of renal metabolic profiles

UPLC-MS method was used to analyze kidney specimens of rats in positive and negative detection modes. After data pre-processing, a total of 3718 positive-mode features and 8374 negative-mode features were identified and exported into EZinfo statistical analysis software for multivariate statistical analysis. PCA is the most widely used unsupervised clustering or classification method in metabolomics research to obtain an overview of grouping trends. The PCA score plots with QC samples in the two modes are

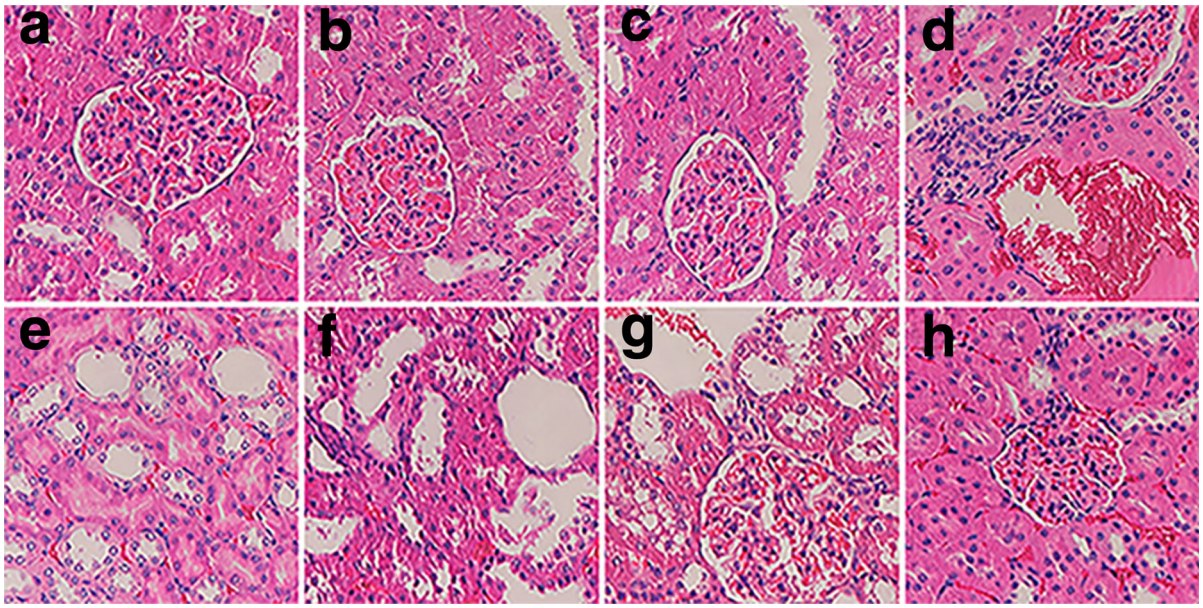

Fig. 1 Histopathological examination of rat kidney sections (hematoxylin and eosin staining, × 400) **a** control group; **b** low-dose quercetin-treated group; **c** high-dose quercetin-treated group; **d–f** Cd-treated group; **g** low-dose quercetin plus Cd-treated group; **h** high-dose quercetin plus Cd-treated group

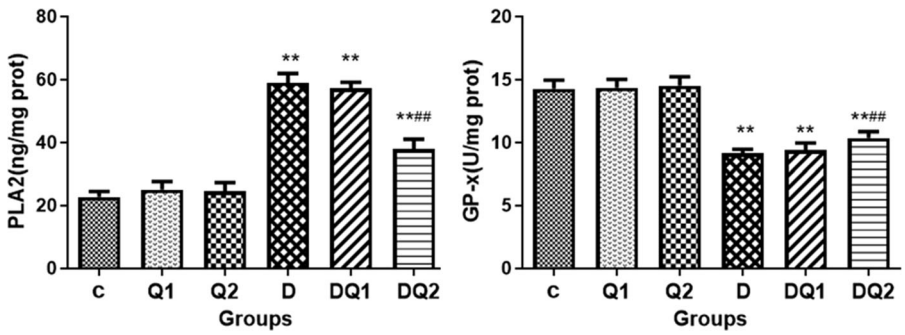

Fig. 2 Activities of PLA2 (left) and GPx (right) in kidney in each group Each bar represents mean ± SD (n = 10). C, control group; Q1, low-dose quercetin-treated group; Q2, high-dose quercetin-treated group; D, Cd-treated group; DQ1, low-dose quercetin plus Cd-treated group; DQ2, high-dose quercetin plus Cd-treated group. *$p < 0.05$ vs. C group (one-way ANOVA). **$p < 0.01$ vs. C group (one-way ANOVA). $^{\#}p < 0.05$ vs. D group (one-way ANOVA). $^{\#\#}p < 0.01$ vs. D group (one-way ANOVA)

displayed in Fig. S3. Four samples outside the limits imposed by the Hotelling's T^2 95% probability ellipse were not excluded and included for subsequent supervised analysis. QC samples (sea green inverted triangles) showed relatively close clustering. To evaluate the instrument stability, six ions extracted from chromatographic peaks of the QC samples (m/z 193.5362, 269.4295, 287.4005, 332.1955, 483.8842, 592.3246 in the positive mode) were randomly selected. The relative standard deviations (RSDs) of peak strength, retention time and m/z were 0.19%—1.55%, 0.06%—2.21% and 0.13%—0.28%, respectively. The results demonstrate that the method has good stability and reproducibility. The loading plots (Fig. S4) seem to suggest that m/z 168.0278, 176.0678, 136.0382, 266.3758, 283.0663, 303.2315, 505.9918, 251.0785, 514.2859, 208.0627 and 173.0575 each aid to separate treatment groups from the control group. These potential biomarkers are far from origin in the loading plot. The PLS-DA score

plots (Fig. 3) showed that group C and D, group DQ2 and D were significantly separated, indicating that Cd could cause nephrotoxicity, and high-dose quercetin (50 mg/kg·bw/day) influenced Cd-induced nephrotoxicity. Additionally, the permutation test and rigorous cross-validation were presented to validate the model and avoid over-fitting. The performance of 200 iterations was shown in Fig. S5. In positive mode, the R2Y and Q2 (predictive ability) were 0.998 and 0.979, respectively. In negative mode, the values of R2Y, Q2 were 0.986 and 0.911, respectively. The Q2 regression line (blue color) had a negative intercept, while the R2 regression line (green color) had a positive intercept. All the permuted values on the left were lower than the original point on the right. All the above indicated that the model was suitable for identification analysis. Besides, the results of the cross-validation ANOVA analysis showed that the PLS-DA model was highly significant (Tables S1 and S2).

Identification and validation of the kidney metabolites

Twenty-one metabolites, including ten in the positive mode and eleven in the negative mode, were initially identified by using Progenesis QI. Considering the retention time, m/z, and fragmentation information with standard substances, we finally identified eleven metabolites (4 positive modes and 7 negative modes). The MS/MS spectra of these metabolites are shown in Figs. S6 and S7. The retention times, m/z, and fragment information of the 11 metabolites are shown in Table 2 and Table S3, respectively. The intensities of metabolites in the kidney of rats under the positive and negative modes are shown in Fig. 4. Compared with group C, the intensities of uric acid (UA), hypoxanthine (Hyp), xanthosine, deoxyinosine (DI), 12-hydroxyeicosatetraenoic acid (tetranor 12-HETE), guanidinosuccinic acid (GSA), taurocholic acid (TCA), hydroxyphenylacetylglycine (HPAG), and ATP in group D significantly up-regulated ($p < 0.00067$), the intensities of formiminoglutamic acid (FIGLU) and arachidonic acid (AA) in group D down-regulated significantly ($p < 0.00067$). When high-dose quercetin along with Cd were administered to rats simultaneously, the intensities of the above 11 metabolites were significantly restored ($p < 0.0033$ or $p < 0.00067$), but there were still statistical differences from those in group C ($p < 0.0033$ or $p < 0.00067$). There were no statistical differences in the intensities of 11 metabolites among C, Q1 and Q2 groups and between D and DQ1 groups ($p > 0.0033$). The ROC curve was carried out to evaluate the specificity and sensitivity of the identified potential metabolites. The results of the ROC curve analysis are presented in Fig. 5. The AUC values of the 11 metabolites are between 0.9 and 1 within a 95% confidence interval, indicating good predictive performances for the identified potential metabolites.

Discussion

In this study, nephrotoxicity induced by Cd and the possible protective effects of quercetin were studied

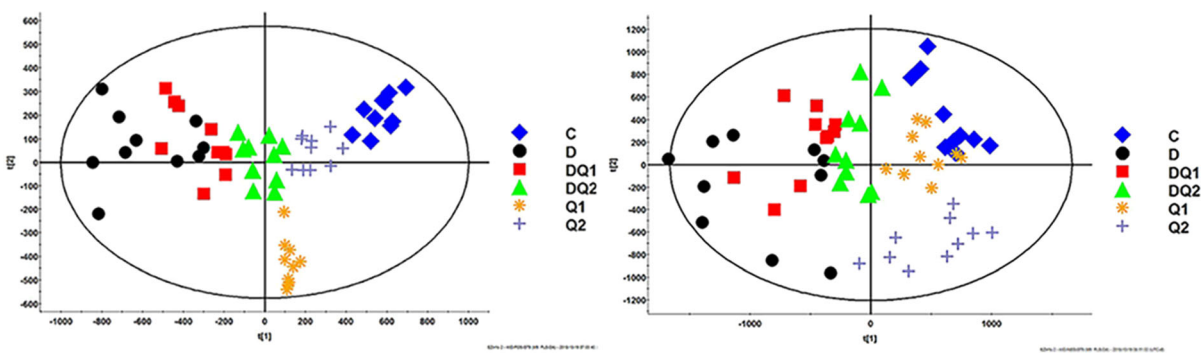

Fig. 3 PLS-DA score plots in the positive (left) and negative mode (right) Black dots: Cd-treated group (D); Red squares: low-dose quercetin plus Cd-treated group (DQ1); Green triangles: high-dose quercetin plus Cd-treated group (DQ2); Blue diamonds: control group (C); Orange stars: low-dose quercetin-treated group (Q1); Purple crosses: high-dose quercetin-treated group (Q2); Ellipse: Hotelling's T^2 (95% confidence region). N = 10

Table 2 Potential metabolites in positive and negative modes

RT (min)	Measured mass (Da)	Calculated mass (Da)	Error (Da)	Elemental composition	Scan mode	Metabolites
6.92	514.2844	514.2839	0.0005	$C_{26}H_{45}NO_7S$	−	TCA[a,b]
2.37	208.0613	208.0610	0.0003	$C_{10}H_{11}NO_4$	−	HPAG[a,b]
1.42	173.0570	173.0563	0.0007	$C_6H_{10}N_2O_4$	−	FIGLU[b]
2.51	251.0790	251.0781	0.0009	$C_{10}H_{12}N_4O_4$	−	Deoxyinosine[a,b]
3.06	505.9883	505.9879	0.0004	$C_{10}H_{16}N_5O_{13}P_3$	−	ATP[a,b]
11.4	303.2329	303.2324	0.0005	$C_{20}H_{32}O_2$	−	AA[a,b]
1.34	283.0689	283.0679	0.0010	$C_{10}H_{12}N_4O_6$	−	Xanthosine[a,b]
1.18	169.0363	169.0361	0.0002	$C_5H_4N_4O_3$	+	UA[a,b]
7.63	176.0675	176.0671	0.0004	$C_5H_9N_3O_4$	+	GSA[a,b]
2.07	137.0469	137.0463	0.0006	$C_5H_4N_4O$	+	Hyp[a,b]
0.66	267.1971	267.1960	0.0011	$C_{16}H_{26}O_3$	+	Tetranor 12-HETE[a,b]

RT retention time, *ATP* adenosine triphosphate, *AA* arachidonic acid, *FIGLU* formiminoglutamic acid, *GSA* guanidinosuccinic acid, *TCA* taurocholic acid, *HPAG* hydroxyphenylacetylglycine, *UA* uric acid, *Hyp* hypoxanthine, *Tetranor 12-HETE* 12-hydroxyeicosatetraenoic acid

[a]The metabolites were identified by comparison to the standards

[b]The metabolites were identified by comparison to the metabolites of the Human Metabolome Database (HMDB)

by metabolomics. Eleven metabolites were finally confirmed (Table 2). Through the information obtained from MetaboAnalyst, HMDB and KEGG database, the metabolic pathway network was drawn to interpret the relationship of potential metabolites/biomarkers and the protective effects of quercetin on Cd-induced nephrotoxicity (Fig. 6).

The first pathway involves lipid metabolism (Fig. 6). TCA is a kind of bile acids (BAs) and produced by the combination of cholic acid and taurine. Cholic acid is produced by cholesterol in the liver under the action of cholesterol-7α-hydroxylase (CYP7A1). BAs biosynthesis is the most crucial pathway for the liver to degrade cholesterol. As the final product of cholesterol catabolism, BAs have much potential toxicity (such as membrane destruction) (Davis et al. 2002). The effects of BAs on the cell membranes are induced by binding with the cell membrane components. As BAs concentrations increased, binding to the membranes also increased, which leads to the destruction of cell membranes integrity, subsequently lysis of hepatocytes and then plays a certain role in the pathogenesis of the cholestatic liver disease (Perez and Briz 2009). The kidney, as an important organ of the urinary system, is thought to play a minor role in BAs excretion. In clinical and animal model studies of chronic renal failure (CRF), elevated levels of BAs are associated with changes in BAs homeostasis. The possible mechanism is reduced filtration of BAs in the kidney (Chu et al. 2015).

It has been reported that BAs can stimulate membrane enzymes (such as PLA2) leading to increased endogenous AA release (Cocco et al. 1999). In our study, the abnormal change in AA intensity may be due to enhanced PLA2 activity, and the hypothesis was confirmed by the determination of PLA2 activity in the kidney (Fig. 2). Meanwhile, the intensity of TCA in group D was significantly higher than that in group C, suggesting that cadmium could cause BAs metabolism disorders in liver and kidney. When high-dose quercetin along with Cd were given to rats simultaneously, TCA intensity significantly decreased (Fig. 4), indicating that quercetin influenced cadmium-induced BAs metabolism disorders. Possible protective mechanism is that quercetin reduces oxidative damage by inhibiting the production of excessive ROS. In addition, quercetin can also protect the kidney by reducing the increase of total cholesterol (TC) levels (Hu et al. 2012).

AA is a ω-6 polyunsaturated fatty acid (PUFA) found mainly in cell membrane phospholipids. When cells are stimulated, AA is released from the phospholipids by PLA2. Previous studies have shown that

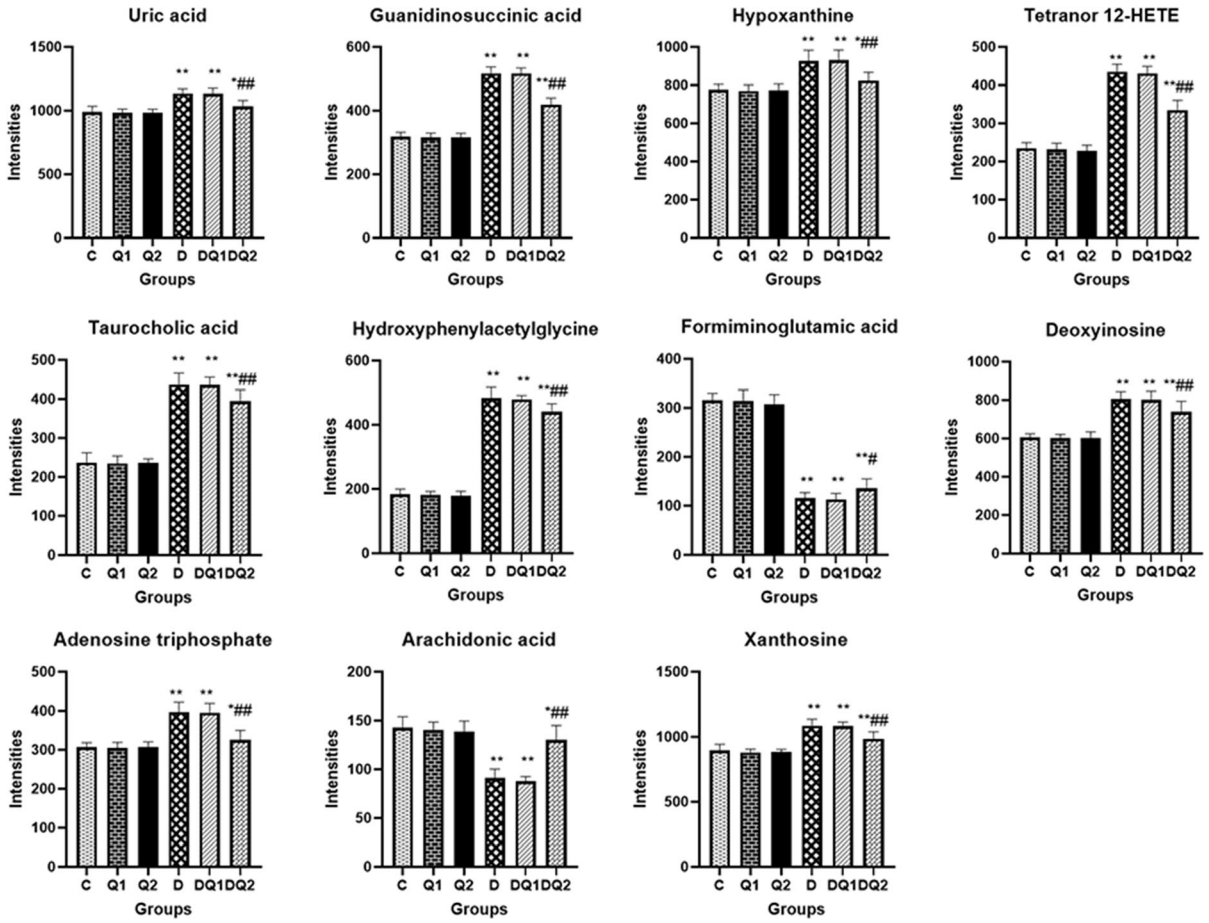

Fig. 4 Intensities of metabolites identified in the positive and negative modes Each bar represents mean ± SD (n = 10). C, control group; Q1, low-dose quercetin-treated group; Q2, high-dose quercetin-treated group; D, Cd-treated group; DQ1, low-dose quercetin plus Cd-treated group; DQ2, high-dose quercetin plus Cd-treated group. *$p < 0.0033$ vs. C group (one-way ANOVA). **$p < 0.00067$ vs. C group (one-way ANOVA). $^{\#}p < 0.0033$ vs. D group (one-way ANOVA). $^{\#\#}p < 0.00067$ vs. D group (one-way ANOVA)

AA has anti-oxidative and anti-inflammatory effects (Qu et al. 2018). AA metabolism disorders can lead to renal vascular injury and end-stage renal disease, and are closely linked to the occurrence, development, and regression of renal inflammation (Imig 2006; Xu et al. 2006). AA is converted to tetranor 12-HETE via the lipoxygenases (LOXs) pathway. Tetranor 12-HETE, an important component of renal disease, has been widely studied. It involves apoptosis induced by oxidative stress and is regarded as a key factor in diabetes-related nephropathy and glomerulonephritis (Manega et al. 2019). Under oxidative stress, decreased GPx activity has been reported to promote the formation of 12-HpETE (the precursor of tetranor 12-HETE), which further aggravates renal injury (Wang et al. 2019). In the current study, AA intensity and GPx activity significantly decreased while tetranor 12-HETE intensity increased in group D compared with those in group C (Figs. 2 and 4). It suggests that cadmium can cause renal AA metabolism disorder. When high-dose quercetin along with Cd were given to rats simultaneously, intensities of above substances recovered obviously, which indicates that quercetin can prevent cadmium-induced renal injury. A possible protective mechanism is that quercetin effectively regulates enzyme activities (such as PLA2, GPx), thereby preventing AA from generating a series of pro-inflammatory eicosanoids and potentially toxic ROS (Al-Asmari et al. 2018; Nanda et al. 2007). The

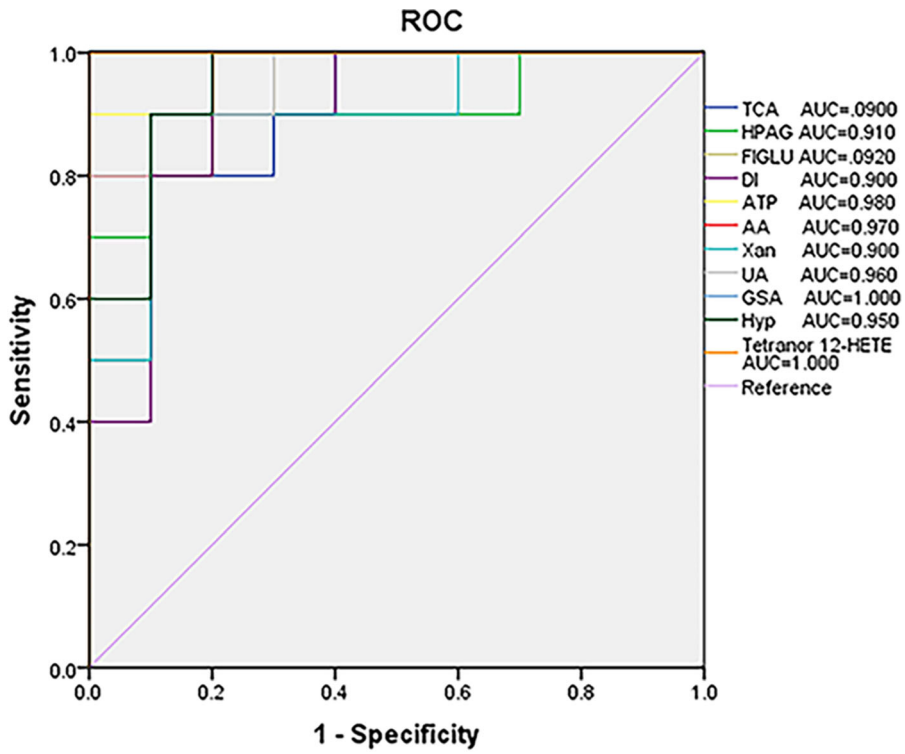

Fig. 5 ROC curve analysis for discrimination of control group and treatment groups for the 11 metabolites

results of renal histopathology (Fig. 1) further supported the above metabolomics results.

The second pathway involves amino acid metabolism (Fig. 6). HPAG is an arylglycines (AGs) and can be derived from the metabolism of tyramine. AGs are also secondary metabolites of fatty acids and often used to diagnose diseases associated with mitochondrial fatty acid β-oxidation (Liu et al. 2018). In addition, AGs can be utilized to diagnose a variety of inborn errors of metabolism (IEM), such as leucine catabolism abnormalities and other enzyme defects in isoleucine, valine, and lysine catabolism (Bonafé et al. 2000). Therefore, the identification of AGs is important for the diagnosis of fatty acid and amino acid metabolism disorders. In the current study, the intensity of HPAG significantly increased in group D compared with group C (Fig. 4), which may be due to the interference of Cd on tyrosine metabolism in the body, leading to mitochondrial fatty acid oxidation disorder, further impairing the kidney. When Cd was given to rats with high-dose quercetin simultaneously, the intensity of HPAG significantly decreased, indicating that quercetin influenced cadmium-induced tyrosine metabolism disorders. Possible protective mechanisms are that quercetin can improve mitochondria function and enzymes antioxidant activities, further protect fatty acid β-oxidation (Sun et al. 2015).

FIGLU is the principal metabolite of histidine degradation. Histidine is transformed to FIGLU and then to glutamate in mammalian tissues. The conversion of FIGLU to glutamate requires tetrahydrofolate (THFA) from folate as a coenzyme. Human urine usually contains only a very small amount of FIGLU. If the function of THFA is interfered, excessive excretion of FIGLU results in the formation of plenty of histamine by decarboxylase catalyzing histidine. Histamine affects glomerular hyperfiltration and tubular reabsorption, which leads to tubular hypertrophy, eventually to glomerulosclerosis and tubular atrophy (Pini et al. 2019). In addition, studies have shown that aspartate (ASP) and glutamate mobilize plasma histamine in the form of neutral metal complexes to further promote histamine catabolism (Berthon and Germonneau 1982). In our study, the intensity of FIGLU in group D significantly decreased compared with group C (Fig. 4), indicating cadmium can cause

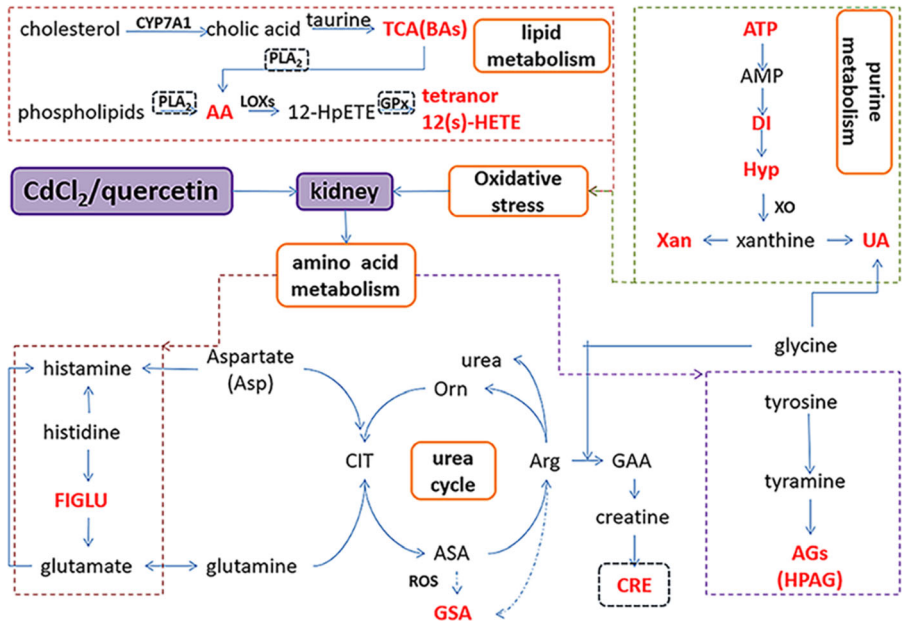

Fig. 6 Metabolic pathways in response to CdCl2 and/or quercetin treatment. *ATP* adenosine triphosphate; *AA* arachidonic acid; *ASA* argininosuccinic acid; *ARG* arginine; *CRE* creatinine; *CIT* citrulline; *CYP7A1* cholesterol-7α-hydroxylase; *DI* deoxyinosine; *FIGLU* formiminoglutamic acid; *GSA* guanidinosuccinic acid; *GAA* guanidinoacetic acid; *GPx* glutathione peroxidase; *HPAG* hydroxyphenylacetylglycine; *Hyp* hypoxanthine; *LOXs* lipoxygenases; *Orn* ornithine; *PLA2* phospholipase A2; *ROS* reactive oxygen species; *TCA* taurocholic acid; *Tetranor 12-HETE* 12-hydroxyeicosatetraenoic acid; *UA* uric acid; *Xan* xanthosine; *XO* xanthine oxidase

histidine metabolism disorder. When Cd and quercetin were given to rats simultaneously, the intensity of FIGLU significantly increased, indicating that quercetin can regulate abnormal histidine metabolism induced by Cd. The possible protective mechanism is that quercetin promotes the absorption of folate, inhibits the release of histamine, and further increases the conversion of histidine to glutamate (Keating et al. 2008; Mlcek et al. 2016).

GSA is one of the earliest uremic toxins found. Under the condition of uremia or renal insufficiency, abnormal urea cycle occurs. The increase of urea and the inhibition of argininosuccinate lyase (ASL) activities lead to argininosuccinic acid (ASA) generate GSA under the action of ROS (Aoyagi et al. 2001). Meanwhile, due to the accumulation of CRE, arginine (ARG) generates GSA under the action of aminotransferase. GSA is a normal metabolism product and usually present in small amounts in the body. The cytotoxicity of GSA has been proved in many systems, the most obvious is to inhibit the activation of platelet factor 3 (PF-3) (Horowitz et al. 1970). Thus, GSA levels can explain many uremia platelet dysfunctions and may be a major factor in uremia hemorrhagic syndrome. In the current study, the intensity of GSA and the level of CRE in group D were significantly higher than those in group C, suggesting that cadmium could cause an abnormal urea cycle. When Cd and quercetin were both given to rats, the intensity of GSA and CRE level significantly decreased (Table 1 and Fig. 4), indicating that quercetin could regulate the above abnormalities induced by Cd. A possible protective mechanism is that quercetin regulates urea cycle disorders by increasing the expression of urea cycle enzymes and blocks GSA production by scavenging free radicals (Kanimozhi et al. 2017).

The third pathway involves purine metabolism (Fig. 6). Oxidative stress is closely linked to the disorder of purine metabolism. Metabolites including ATP, DI, Hyp, xanthosine and UA are involved in the purine pathway. DI was found to be associated with a deficiency of purine nucleoside phosphorylase. Hyp is a metabolite of energy-rich phosphorylated nucleotide ATP and is also a uremic toxin. Potentially harmful free radicals are released when Hyp combines with xanthine oxidase (XO) and oxygen to form xanthine

and UA, which may be important for the occurrence of ischemic renal injury (Mraz et al. 2015). Therefore, Hyp levels are closely related to free radicals' formation. UA, as an oxidative product of purine metabolism, has also been identified as a uremia toxin. Elevated UA levels can lead to hyperuricemia. Chronic hyperuricemia is closely linked to renal disease and caused by decreased glomerular filtration rate (GFR) and urate excretion, or increased overall tubular absorption. In glomerular lesions and tubular damage, purine metabolism enhances, the decrease of UA filtration and urinary output lead to an increase of serum UA. Elevated serum UA levels can lead to the deposition of urate crystals, and ultimately cause chronic joint inflammation, urate/xanthine calculus and kidney damage (Lang et al. 2019). In our study, the intensities of the renal purine metabolites (ATP, DI, Hyp, xanthosine, UA, etc.) and serum UA level in group D were significantly higher than those in group C (Table 1 and Fig. 4), which may be related to Cd-induced oxidative stress. When Cd and quercetin were both given to rats, the intensities of purine metabolites and serum UA level decreased significantly, which indicates quercetin may prevent nephrotoxicity induced by Cd from inhibition of oxidative stress. In addition, cadmium concentration of group DQ2 significantly decreased compared with that of group D (Fig. S2), which may be related to the suppression of quercetin on Cd accumulation in the kidneys. It is likely that quercetin (i) chelated Cd and/or (ii) improved renal function in Cd-exposed rats by lowering oxidative stress in the kidneys, thus increasing CRE and Cd clearance, and enhancing Cd excretion through the kidneys (Badr et al. 2019; Nna et al. 2017). The results further supported the above metabolomics results.

The kidney is an important organ that produces urine and removes waste metabolites and toxins from the body. Therefore, some metabolites in the urine can reflect kidney damage. In our previous study, the metabolomics analysis of urine showed the renal damage caused by Cd (Liu et al. 2019). Therefore, a statistical correlation analysis of metabolites between urine and kidney was conducted (Fig. S8). Allantoic acid, as a final product of UA degradation, is also involved in major pathways of purine metabolism (Cai et al. 2017). The purine metabolites (ATP, DI, Hyp, xanthine, and UA) in the kidneys were positively correlated with allantoic acid in urine and negatively correlated with UA in urine, further supporting that the renal purine metabolites are related to oxidative stress caused by Cd. Taurine in urine showed a strong negative correlation with TCA in the kidneys, indicating that Cd may interfere with the BAs metabolism. LysoPC can generate active species by activating the 5-lipoxygenase pathway and induce the enhancement of oxidative stress. In addition, LysoPC increases the release of AA by activating PLA2 (Oestvang et al. 2011). As mentioned above, LysoPC in urine was negatively correlated with AA in kidneys, suggesting that Cd may interfere with lipids metabolism.

Conclusions

This research explored the protective effects of quercetin on the Cd-induced nephrotoxicity utilizing metabolomics technology. The results indicated that quercetin may have protective effects on Cd-induced nephrotoxicity by enhancing the antioxidant defense system of the body and regulating the metabolism of lipids, amino acids, and purine.

Acknowledgments We are particularly grateful to the Laboratory of Nutrition and Food Hygiene in Harbin Medical University, which is the key laboratory of Heilongjiang Province and Heilongjiang Higher Education Institutions.

Author contributions XJZ and CC conceived and supervised the study. TG, KZ, RJW, and XZ performed the experimental work. SQJ and SQL collected the data. TG and YWX analyzed the data. TG wrote and revised the manuscript. All authors read and approved the manuscript.

Funding The author(s) disclosed that they had received financial support for the research, authorship and/or publication of this article from the China National Centre for Food Safety Risk Assessment.

Compliance with ethical standards

Conflict of interest The authors declare that they have no conflicts of interest.

Ethical approval The whole animal experiment process conformed to the guide for the care and use of laboratory animals of Harbin Medical University (Heilongjiang, China), and had been approved by the medical ethics committee of Harbin Medical University.

References

Al-Asmari AK, Khan HA, Manthiri RA, Al-Khlaiwi AA, Al-Asmari BA, Ibrahim KE (2018) Protective effects of a natural herbal compound quercetin against snake venom-induced hepatic and renal toxicities in rats. Food Chem Toxicol 118:105–110. https://doi.org/10.1016/j.fct.2018.05.016

Aoyagi K et al (2001) Role of nitric oxide in the synthesis of guanidinosuccinic acid, an activator of the N-methyl-D-aspartate receptor. Kidney Int Suppl 78:S93–S96. https://doi.org/10.1046/j.1523-1755.2001.59780093.x

Badr GM et al (2019) Protective effects of quercetin supplementation against short-term toxicity of cadmium-induced hematological impairment, hypothyroidism, and testicular disturbances in albino rats. Environ Sci Pollut Res Int 26:8202–8211. https://doi.org/10.1007/s11356-019-04276-1

Bartholomew CJ, Li N, Li Y, Dai W, Nibagwire D, Guo T (2020) Characteristics and health risk assessment of heavy metals in street dust for children in Jinhua, China. Environ Sci Pollut Res Int 27:5042–5055. https://doi.org/10.1007/s11356-019-07144-0

Berthon G, Germonneau P (1982) Histamine as a ligand in blood plasma. Part 6. Aspartate and glutamate as possible partner ligands for zinc and histamine to favour histamine catabolism. Agents Actions 12:619–629. https://doi.org/10.1007/bf01965070

Bonafé L, Troxler H, Kuster T, Heizmann CW, Chamoles NA, Burlina AB, Blau N (2000) Evaluation of urinary acylglycines by electrospray tandem mass spectrometry in mitochondrial energy metabolism defects and organic acidurias. Mol Genet Metab 69:302–311. https://doi.org/10.1006/mgme.2000.2982

Cai HL et al (2017) Therapeutic efficacy of atypical antipsychotic drugs by targeting multiple stress-related metabolic pathways. Transl Psychiatry 7:e1130. https://doi.org/10.1038/tp.2017.94

Chen S, Zhang M, Bo L, Li S, Hu L, Zhao X, Sun C (2018) Metabolomic analysis of the toxic effect of chronic exposure of cadmium on rat urine. Environ Sci Pollut Res Int 25:3765–3774. https://doi.org/10.1007/s11356-017-0774-8

Chu L, Zhang K, Zhang Y, Jin X, Jiang H (2015) Mechanism underlying an elevated serum bile acid level in chronic renal failure patients. Int Urol Nephrol 47:345–351. https://doi.org/10.1007/s11255-014-0901-0

Cocco T, Di Paola M, Papa S, Lorusso M (1999) Arachidonic acid interaction with the mitochondrial electron transport chain promotes reactive oxygen species generation. Free Radic Biol Med 27:51–59. https://doi.org/10.1016/s0891-5849(99)00034-9

Davis RA, Miyake JH, Hui TY, Spann NJ (2002) Regulation of cholesterol-7alpha-hydroxylase: BAREly missing a SHP. J Lipid Res 43:533–543

Djordjevic VR et al (2019) Environmental cadmium exposure and pancreatic cancer: Evidence from case control, animal and in vitro studies. Environ Int 128:353–361. https://doi.org/10.1016/j.envint.2019.04.048

Feng J, Liu H, Bhakoo KK, Lu L, Chen Z (2011) A metabonomic analysis of organ specific response to USPIO administration. Biomaterials 32:6558–6569. https://doi.org/10.1016/j.biomaterials.2011.05.035

García-Sevillano MA, García-Barrera T, Navarro F, Montero-Lobato Z, Gómez-Ariza JL (2015) Shotgun metabolomic approach based on mass spectrometry for hepatic mitochondria of mice under arsenic exposure. Biometals 28:341–351. https://doi.org/10.1007/s10534-015-9837-9

Ghosh K, Indra N (2018) Cadmium treatment induces echinocytosis, DNA damage, inflammation, and apoptosis in cardiac tissue of albino Wistar rats. Environ Toxicol Pharmacol 59:43–52. https://doi.org/10.1016/j.etap.2018.02.009

Griffin JL (2020) Twenty years of metabonomics: so what has metabonomics done for toxicology? Xenobiotica 50:110–114. https://doi.org/10.1080/00498254.2019.1697015

Horowitz HI, Stein IM, Cohen BD, White JG (1970) Further studies on the platelet-inhibitory effect of guanidinosuccinic acid and its role in uremic bleeding. Am J Med 49:336–345. https://doi.org/10.1016/s0002-9343(70)80025-0

Hu L, Bo L, Zhang M, Li S, Zhao X, Sun C (2018) Metabonomics analysis of serum from rats given long-term and low-level cadmium by ultra-performance liquid chromatography-mass spectrometry. Xenobiotica 48:1079–1088. https://doi.org/10.1080/00498254.2017.1397811

Hu Q-H, Zhang X, Pan Y, Li Y-C, Kong L-D (2012) Allopurinol, quercetin and rutin ameliorate renal NLRP3 inflammasome activation and lipid accumulation in fructose-fed rats. Biochem Pharmacol 84:113–125. https://doi.org/10.1016/j.bcp.2012.03.005

Imig JD (2006) Eicosanoids and renal vascular function in diseases. Clin Sci (Lond) 111:21–34. https://doi.org/10.1042/CS20050251

Järup L, Akesson A (2009) Current status of cadmium as an environmental health problem. Toxicol Appl Pharmacol 238:201–208. https://doi.org/10.1016/j.taap.2009.04.020

Jia S, Guan T, Zhang X, Liu Y, Liu Y, Zhao X (2020) Serum metabonomics analysis of quercetin against the toxicity induced by cadmium in rats. J Biochem Mol Toxicol. https://doi.org/10.1002/jbt.22448

Joardar S, Dewanjee S, Bhowmick S, Dua TK, Das S, Saha A, De Feo V (2019) Rosmarinic acid attenuates cadmium-induced nephrotoxicity via inhibition of oxidative stress, apoptosis, inflammation and fibrosis. Int J Mol Sci 20:2027. https://doi.org/10.3390/ijms20082027

Kanimozhi S, Subramanian P, Shanmugapriya S, Sathishkumar S (2017) Role of bioflavonoid quercetin on expression of urea cycle enzymes, astrocytic and inflammatory markers in hyperammonemic rats. Indian J Clin Biochem 32:68–73. https://doi.org/10.1007/s12291-016-0575-8

Keating E, Lemos C, Gonçalves P, Martel F (2008) Acute and chronic effects of some dietary bioactive compounds on folic acid uptake and on the expression of folic acid transporters by the human trophoblast cell line BeWo. J Nutr Biochem 19:91–100. https://doi.org/10.1016/j.jnutbio.2007.01.007

Lamtai M, Azirar S, Zghari O, Ouakki S, El Hessni A, Mesfioui A, Ouichou A (2020) Melatonin ameliorates cadmium-induced affective and cognitive impairments and hippocampal oxidative stress in rat. Biol Trace Elem Res. https://doi.org/10.1007/s12011-020-02247-z

Lang S et al (2019) A conserved role of the insulin-like signaling pathway in diet-dependent uric acid pathologies in Drosophila melanogaster. PLoS Genet 15:e1008318. https://doi.org/10.1371/journal.pgen.1008318

Liu H, Zhou Y, Wang J, Xiong C, Xue J, Zhan L, Nie Z (2018) N-Phenyl-2-naphthylamine as a novel MALDI matrix for analysis and in situ imaging of small molecules. Anal Chem 90:729–736. https://doi.org/10.1021/acs.analchem.7b02710

Liu Y, Zhang X, Guan T, Jia S, Liu Y, Zhao X (2019) Effects of quercetin on cadmium-induced toxicity in rat urine using metabonomics techniques. Hum Exp Toxicol. https://doi.org/10.1177/0960327119895811

Manega CM et al (2019) 12(S)-Hydroxyeicosatetraenoic acid downregulates monocyte-derived macrophage efferocytosis: New insights in atherosclerosis. Pharmacol Res 144:336–342. https://doi.org/10.1016/j.phrs.2019.03.012

Mao T et al (2018) Protective effects of quercetin against cadmium chloride-induced oxidative injury in goat sperm and zygotes. Biol Trace Elem Res 185:344–355. https://doi.org/10.1007/s12011-018-1255-8

Mlcek J, Jurikova T, Skrovankova S, Sochor J (2016) Quercetin and its anti-allergic immune response. Molecules (Basel, Switzerland) 21:623. https://doi.org/10.3390/molecules21050623

Mraz M, Hurba O, Bartl J, Dolezel Z, Marinaki A, Fairbanks L, Stiburkova B (2015) Modern diagnostic approach to hereditary xanthinuria. Urolithiasis 43:61–67. https://doi.org/10.1007/s00240-014-0734-4

Nanda BL, Nataraju A, Rajesh R, Rangappa KS, Shekar MA, Vishwanath BS (2007) PLA2 mediated arachidonate free radicals: PLA2 inhibition and neutralization of free radicals by anti-oxidants–a new role as anti-inflammatory molecule. Curr Top Med Chem 7:765–777. https://doi.org/10.2174/156802607780487623

Nna VU, Ujah GA, Mohamed M, Etim KB, Igba BO, Augustine ER, Osim EE (2017) Cadmium chloride-induced testicular toxicity in male wistar rats; prophylactic effect of quercetin, and assessment of testicular recovery following cadmium chloride withdrawal. Biomed Pharmacother 94:109–123. https://doi.org/10.1016/j.biopha.2017.07.087

Oestvang J, Anthonsen MW, Johansen B (2011) LysoPC and PAF trigger arachidonic acid release by divergent signaling mechanisms in monocytes. J Lipids 2011:532145. https://doi.org/10.1155/2011/532145

Ou Q, Zheng Z, Zhao Y, Lin W (2020) Impact of quercetin on systemic levels of inflammation: a meta-analysis of randomised controlled human trials. Int J Food Sci Nutr 71:152–163. https://doi.org/10.1080/09637486.2019.1627515

Perez M-J, Briz O (2009) Bile-acid-induced cell injury and protection. World J Gastroenterol 15:1677–1689. https://doi.org/10.3748/wjg.15.1677

Pingili RB, Challa SR, Pawar AK, Toleti V, Kodali T, Koppula S (2020) A systematic review on hepatoprotective activity of quercetin against various drugs and toxic agents: Evidence from preclinical studies. Phytother Res 34:5–32. https://doi.org/10.1002/ptr.6503

Pini A, Verta R, Grange C, Gurrieri M, Rosa AC (2019) Histamine and diabetic nephropathy: an up-to-date overview. Clin Sci (Lond) 133:41–54. https://doi.org/10.1042/CS20180839

Qu Y, Zhang HL, Zhang XP, Jiang HL (2018) Arachidonic acid attenuates brain damage in a rat model of ischemia/reperfusion by inhibiting inflammatory response and oxidative stress. Hum Exp Toxicol 37:135–141. https://doi.org/10.1177/0960327117692134

Roy S, Banerjee S, Chakraborty T (2018) Vanadium quercetin complex attenuates mammary cancer by regulating the P53, Akt/mTOR pathway and downregulates cellular proliferation correlated with increased apoptotic events. Biometals 31:647–671. https://doi.org/10.1007/s10534-018-0117-3

Su G, Wang H, Bai J, Chen G, Pei Y (2019) A metabonomics approach to drug toxicology in liver disease and its application in traditional Chinese medicine. Curr Drug Metab 20:292–300. https://doi.org/10.2174/1389200220666181231124439

Sun X, Yamasaki M, Katsube T, Shiwaku K (2015) Effects of quercetin derivatives from mulberry leaves: Improved gene expression related hepatic lipid and glucose metabolism in short-term high-fat fed mice. Nutr Res Pract 9:137–143. https://doi.org/10.4162/nrp.2015.9.2.137

Sun Y, Zhou Q, Zheng J (2019) Nephrotoxic metals of cadmium, lead, mercury and arsenic and the odds of kidney stones in adults: an exposure-response analysis of NHANES 2007–2016. Environ Int 132:105115. https://doi.org/10.1016/j.envint.2019.105115

Tian J, Hu J, He W, Zhou L, Huang Y (2020) Parental exposure to cadmium chloride causes developmental toxicity and thyroid endocrine disruption in zebrafish offspring. Comp Biochem Physiol C 234:108782. https://doi.org/10.1016/j.cbpc.2020.108782

Turner A (2019) Cadmium pigments in consumer products and their health risks. Sci Total Environ 657:1409–1418. https://doi.org/10.1016/j.scitotenv.2018.12.096

Wang T, Fu X, Chen Q, Patra JK, Wang D, Wang Z, Gai Z (2019) Arachidonic acid metabolism and kidney inflammation. Int J Mol Sci 20:3683. https://doi.org/10.3390/ijms20153683

Xu MY, Wang P, Sun YJ, Wu YJ (2019a) Disruption of kidney metabolism in rats after subchronic combined exposure to low-dose cadmium and chlorpyrifos. Chem Res Toxicol 32:122–129. https://doi.org/10.1021/acs.chemrestox.8b00219

Xu Y et al (2019b) Metabolomics characterizes the effects and mechanisms of quercetin in nonalcoholic fatty liver disease development. Int J Mol Sci. https://doi.org/10.3390/ijms20051220

Xu ZG, Li SL, Lanting L, Kim YS, Shanmugam N, Reddy MA, Natarajan R (2006) Relationship between 12/15-lipoxygenase and COX-2 in mesangial cells: potential role in diabetic nephropathy. Kidney Int 69:512–519. https://doi.org/10.1038/sj.ki.5000137

Zhang L, Dong M, Guangyong X, Yuan T, Tang H, Wang Y (2018) Metabolomics reveals that dietary ferulic acid and quercetin modulate metabolic homeostasis in rats. J Agric

Food Chem 66:1723–1731. https://doi.org/10.1021/acs.jafc.8b00054
Zhang Y et al (2010) Dietary flavonol and flavone intakes and their major food sources in Chinese adults. Nutr Cancer 62:1120–1127. https://doi.org/10.1080/01635581.2010.513800